CONDENSED-STATE PHYSICS

Structure and mechanical properties of (Zr, Nb)N, (Zr, Hf)N and (Zr, Nb, Hf)N coatings

N. N. Cherenda · S. N. Grigoriev · A. V. Basalai · N. V. Bibik · A. A. Vereschaka · A. Yu. Isobello · D. P. Rusalsky · A. K. Kuleshov · V. V. Uglov · V. V. Chayeuski · I. A. Saladukhin

Received: 10 March 2025 / Accepted: 8 April 2025

Abstract
The paper investigates the structure and mechanical properties of (Zr, Nb)N, (Zr, Hf)N and (Zr, Nb, Hf)N vacuum arc deposited coatings on the Ti-6Al-4V titanium substrate. The coatings are a single-phase ZrN-based solid solution. The highest (17 GPa) microhardness is obtained for the (Zr, Hf, Nb)N coating. The (Zr, Hf)N coating shows the highest critical force Lc3 during scratch tests. A decrease in the niobium concentration in the (Zr, Nb)N coating and the higher hafnium concentration in the (Zr, Hf)N coating, provide the growth in the critical force Lc3.

Keywords Titanium alloy · Medical implants · Nitride coating · Adhesion · Microhardness

Introduction

Titanium alloys are the most frequently used material for the production of metal implants applied in various fields of medicine [1–4]. At the same time, implants are foreign objects for a human body and can cause immune and other system's response [2]. For example, the Ti-6Al-4V alloy widely used in the implant production, contains potentially toxic atoms of aluminum and vanadium which have the risk of releasing into the human body [1–3]. Vanadium is associated with a gastrointestinal discomfort, decreased body weight and carcinogenic effect [2]. Aluminium is also toxic in high doses and can cause a number of diseases: neurotoxicity, disordered motor activity, reduction in the spatial memory capacity and Alzheimer's disease [2].

A protective coating deposition is widely used to avoid negative effects [5, 6]. According to Wu *et al*. [7], physical vapor deposition (PVD) of coatings based on transition metal nitrides, attracts considerable attention from researchers. Such coatings possess unique mechanical and tribological properties and good corrosion resistance. ZrN coatings belong to this type [5, 6, 8]. In particular, ZrN coatings are commercially available for orthopedic implants, which are used for jointed surfaces in arthroplasty [5]. Besides binary nitride materials, ternary and higher-order material systems are being developed to ensure the best combination of properties [9]. Zr-Nb-N and Zr-Hf-N coating compositions are an important issue in this approach [9–17].

In a number of works it is reported that Zr-Nb-N PVD coatings possess the high hardness, high elastic modulus and low wear rate [10–12]. According to [10, 11], the Zr–Nb–N system has a high potential to provide scratch resistant coatings. Many researchers [11, 12], mention the ZrN-based FCC solid solution as a single or the main phase of the coating. At the same time, different Nb concentration leads to structural changes

 https://doi.org/10.1007/s11182-025-03471-7

Published online: 28 May 2025

in the coating, affecting its mechanical properties [12, 13]. Krysina *et al.* [12], report that the Nb addition in the coating results in its structure refinement. The same effect is described by Qian *et al*. [13] for Nb-Zr-N films. The growth in the Zr/Nb stoichiometric ratio provides the increased the average grain size and lattice parameter. Zr-Hf-N coatings also have the FCC crystal structure and are characterized by enhanced mechanical and tribological properties [14–16]. It is also reported that the higher Hf concentration in the coating does not significantly change its hardness. Negligible hardening of the solid solution due to a small difference in the atomic radius of Zr and Hf, can be the main reason of this effect [14]. Atar *et al.* [17] show that residual stresses in (Zr, Hf)N films with 11.9 at.% Hf, are induced by the small difference in the atomic radius. In contrast, the growth in the Hf concentration, considerably increases the adhesive strength and wear resistance of coatings [14, 15].

In our recent research [18] into mechanical and corrosion properties of ZrN, (Zr, Ti)N, (Zr, Hf)N, (Zr, Nb)N, (Ti, Zr, Hf)N and (Ti, Zr, Nb)N coatings deposited onto the Ti-6Al-4V titanium substrate, it is shown that the presence of Hf atoms in the coating enhances its hardness and adhesive strength, whereas the addition of Nb atoms provides the high corrosion resistance of the (Ti, Zr, Nb)N coating.

The aim of this work is to study the influence of the Nb and Hf concentration on the structure and mechanical properties of (Zr, Hf)N, (Zr, Nb)N and (Zr, Nb, Hf)N coatings.

Materials and methods

The Ti-6Al-4V titanium alloy (Grade 5) was used as a substrate. The coatings were deposited onto substrates by vacuum arc deposition at the cathode spot motion control in nitrogen using a modernized VIT-2 PVD installation [19]. Prior to the deposition process, the substrate surface was cleaned by Zr ions, resulting in the formation of a thin (~50 nm) metal sublayer. The coatings were deposited using two cathodic vacuum arc evaporators. The following cathode pairs were used: Zr and 50 at.% Zr–50 at.% Nb, Zr and 50 at.% Zr–50 at.% Hf, 50 at.% Zr–50 at.% Nb and 50 at.% Zr–50 at.% Hf. As a result, (Zr, Nb)N, (Zr, Hf)N and (Zr, Nb, Hf)N coatings were deposited. The second Zr cathode allowed to reduce the Nb and Hf concentration in (Zr, Nb)N and (Zr, Hf)N coatings in contrast to those investigated in [19]. The deposition parameters included 80 A arc current of the zirconium cathode, 85 and 90 A arc current of Zr-Nb, Zr-Hf cathodes, respectively, 0.42 Pa gas pressure, –150 V substrate bias voltage, 0.7 rpm rotation speed, and ~4.5 μm coating thickness.

X-ray diffraction patterns (XRD) of the coating structure and phase composition were obtained using a Rigaku Ultima IV X-ray Diffractometer (Japan) equipped with a graphite monochromator with Cu Kα radiation. SEM/EDX elemental analysis was conducted on an LEO 1455VP scanning electron microscope (SEM) (Karl Zeiss, Germany). The microhardness testing was performed on a 402 MVD (Instron Wolpert Wilson Instruments) Vickers hardness tester. Measurements were conducted at 1 N normal load, 10 s exposure. Scratch tests were carried out using Vickers diamond pyramid tip with 0.4 mm radius and linear load increasing from 0.05 to 98 N. The running track length was 15 mm (0.17 kg/s loading speed, 0.19 mm/s motion speed). Three tracks were made for each sample, and the obtained results were averaged.

Results and discussion

The elemental composition of the surface layer ~1 μm thick is presented in Table 1. One can see that zirconium is the predominant metallic element in multicomponent coatings. The use of two cathodes (one of which is Zr) in (Zr, Nb)N and (Zr, Hf)N coatings, provides the reduction in the niobium and hafnium concentration to respectively 10.2 and 2.0 at.% in the ZrN-based solid solution. The use of Zr-Nb or Zr-Hf cathode leads to the formation of (Zr, Nb)N and (Zr, Hf)N coatings with their concentration of 23.5 and 5.7 at.%, respectively [19]. A combination of these data obtained earlier, allows to investigate the effect of niobium and hafnium

Table 1 EDX analysis of the elemental composition of (Zr, Nb)N, (Zr, Hf)N and (Zr, Nb, Hf)N coatings

Coatings	Elemental composition, at.%			
	Zr	Nb	Hf	N
(Zr, Nb)N	41.1	10.2	–	48.7
(Zr, Hf)N	49.4	–	2.0	48.6
(Zr, Nb, Hf)N	38.5	11.5	3.3	46.7

concentration on the coating properties. The Nb and Hf concentration in the (Zr, Nb, Hf)N coating is higher than in (Zr, Nb)N and (Zr, Hf)N coatings. However, this difference is insignificant and near the error limit of the concentration detection. For all types of the coatings, the nitrogen concentration approaches to stoichiometric (47–49 at.%).

Figure 1 shows XRD patterns for substrates with (Zr, Hf)N, (Zr, Nb)N and (Zr, Nb, Hf)N coatings. As can be seen from this figure, earlier obtained patterns are observed in [19]. In particular, the obtained single-phase ZrN-based FCC solid solution coatings comprise additional alloying elements. Diffraction peaks of the ZrN-based FCC solid solution, are broader for (Zr, Nb)N and (Zr, Nb, Hf)N coatings than for the (Zr, Hf)N coating. This can be explained by both the higher coatings microstress and smaller crystallite size. The latter is already observed in [12, 13]. Also, a change is observed for the lattice parameter (calculated by (111) and (311) diffraction peaks) of the ZrN-based solid solution. Calculation results are summarized in Fig. 2.

One can see that the use of the Zr-Nb cathode leads to a decrease in the lattice parameter of the solid solution in the (Zr, Nb)N and (Zr, Nb, Hf)N coatings compared to the (Zr, Hf)N coating. The Nb atomic radius is smaller (0.164 nm) than that of Zr (0.175 nm) that can be a reason for this effect. The similar effect is described in [12]. The lattice parameter of solid solutions corresponds (within the error limits) to the lattice parameter in the ZrN coating [19]. A comparison with these data, shows that a decrease in the hafnium content from 5.7 to 2 at.%, results in a slight growth in the lattice parameter approaching to that of the ZrN coating. At the same time, a decrease in the niobium concentration from 23.5 to 10.2 at.%, results in a significant increase in the lattice parameter matching the ZrN lattice parameter. In general, a decrease in the niobium and hafnium concentration, lead to a decrease in micro and macrostresses in coatings and, consequently, in mechanical properties. The lattice parameter of the solid solution in the (Zr, Nb, Hf)N coating does not differ within the error limits from the lattice parameter of the solid solution in the (Zr, Nb)N coating, which is associated with a slight change in the elemental composition of coatings (see Table 1).

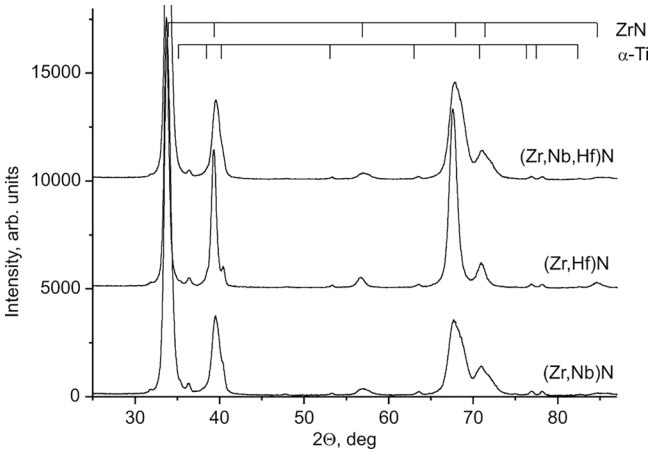

Fig. 1 XRD patterns for samples with (Zr, Nb)N, (Zr, Hf)N and (Zr, Nb, Hf)N coatings

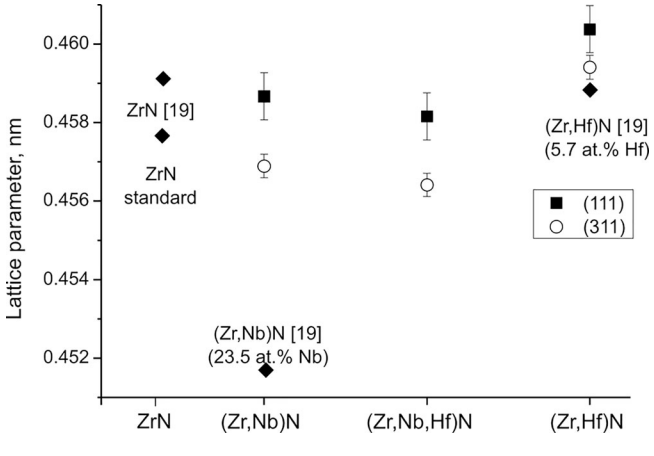

Fig. 2 Lattice parameter of ZrN solid solution in (Zr, Nb)N, (Zr, Hf)N and (Zr, Nb, Hf)N coatings. Lattice parameters taken from [19] are calculated from (111) diffraction peak position of the reference ZrN phase

Vickers microhardness measurements were carried out for (Zr, Nb)N, (Zr, Hf)N and (Zr, Nb, Hf)N coatings at the penetration depth of 1.5–2 μm. The highest (15.8±0.7 GPa and 16.9±1.7 GPa) microhardness was observed for (Zr, Hf)N and (Zr, Nb, Hf)N coatings, which had almost similar elemental composition (Table 1) and, probably, macrostress values (Fig. 2). The microhardness of the (Zr, Nb)N coating was 9.2±0.6 GPa. The obtained data were consistent with those obtained in previous research, where it was found that the (Zr, Nb)N coating microhardness was lower than that of other coatings. This can be associated with tensile stress formation in the coating [18].

The Knoop hardness test was used for the microhardness measurements in [18] for the ZrN coating, (Zr, Nb)N coating with 23.5 at.% Nb and (Zr, Hf)N coating with 5.7 at.% Hf. The obtained microhardness was 21.5, 12.0 and 28.3 GPa, respectively. A direct comparison with the data received in this work, was not correct because different types of indenters and loads were used. However, it is possible to estimate the composition effect on the microhardness through the ratio of the highest (Zr, Hf)N coating microhardness to the lowest microhardness of the (Zr, Nb)N coating. For the case presented in [18], this ratio was 2.4. At the same time, this ratio was reduced to 1.9. Thus, the Nb and Hf content reduction in (Zr, Nb)N and (Zr, Hf)N coatings led to the microhardness ratio reduced to 1, while the microhardness value approached to that of the ZrN coating.

The adhesive strength of the coating was measured after their deposition onto the titanium substrate. All scratches occurred along the direction of the sample grinding. It was found that wear tracks were characterized by chips on the track side and complete coating delamination.

It is known that three main critical loads are usually determined by scratch tests: Lc1 corresponds to the crack initiation, Lc2 denotes the first chipping, and Lc3 indicates complete delamination [20]. In these experiments, the critical load Lc3 is determined by optical microscopy *via* the distance at which complete delamination occurs and the applied load dependence on the sliding distance of the indenter. The load Lc3 is 36 N for samples with the (Zr, Nb)N coating, 50 N for (Zr, Hf)N coating, and 42 N for (Zr, Nb, Hf)N coating.

Another criterion for complete delamination of the coating deposited onto a relatively smooth surface, is probably a critical change in the friction coefficient of the indenter [20]. The dependences between the indenter friction coefficient and sliding distance are shown in Fig. 3. One can see a dramatic growth in the friction coefficient indicating to complete delamination of the coating and the indenter penetration in the Ti-6Al-4V alloy substrate that corresponds to the critical load Lc3 obtained by optical microscopy. The highest critical load Lc3 is observed for Hf-containing coatings. However, these coatings are characterized by the largest chips along the entire track length compared to other coatings.

In the work [18], adhesive strength tests of ZrN, (Zr, Nb)N coatings with 23.5 at.% Nb and (Zr, Hf)N coatings with 5.7 at.% Hf were conducted under the same conditions as in the present work. The critical load values for these coatings were 37.3, 33.4 and 54.0 N, respectively [18]. Comparison with the data obtained in the present

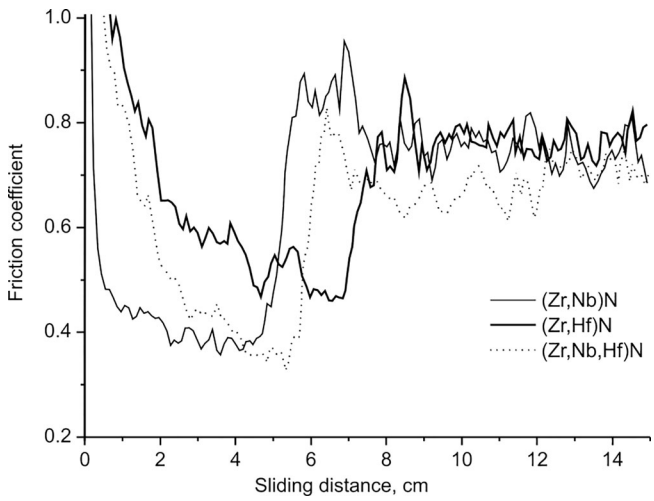

Fig. 3 Dependences between the friction coefficient and sliding distance for (Zr, Nb)N, (Zr, Hf)N and (Zr, Nb, Hf)N coatings

work showed that the lower niobium content in the (Zr, Nb)N coating and the higher hafnium concentration in the (Zr, Hf)N coating enhanced the critical load Lc3. These data correlated with the previous data [18] on the Nb content in the ZrN coating, which caused a decrease in the critical load in adhesive strength tests. That was probably due to the formation of tensile residual stresses in the coating crystal lattice [19], which contributed to the coating delamination under mechanical loads. On the contrary, the Hf content led to an increase in the coating adhesive strength and hardness. A positive influence of Hf atoms on the adhesive strength of ZrN coatings was already detected in [14, 15]. However, a large difference in strength properties of the Ti alloy substrate and the hard coating, resulted in an increase in the coating fragmentation along the scratch. The (Zr, Nb, Hf)N coating had a kind of average mechanical characteristics due to the opposite effect of Nb and Hf atoms on the mechanical properties of ZrN-based coatings.

Conclusions

The structure, elemental composition and mechanical properties were investigated for (Zr, Nb)N, (Zr, Hf)N and (Zr, Nb, Hf)N vacuum arc deposited coatings onto the Ti-6Al-4V titanium substrate. The coatings were single-phase ZrN-based FCC solid solution. Nb-containing coatings had the lower lattice parameter than the ZrN reference phase that was associated with the smaller atomic radius of niobium atoms. Comparison with previously conducted investigations showed that the higher niobium concentration led to a decrease in the lattice parameter of the ZrN-based solid solution.

Vickers microhardness measurements showed that the microhardness of (Zr, Hf)N and (Zr, Nb, Hf)N coatings was the highest and ranged between 16 and 17 GPa. The (Zr, Nb)N coating microhardness was ~9 GPa. During scratch testing, the highest critical load Lc3 was observed for the (Zr, Hf)N coating. However, Hf-containing coatings were characterized by the largest fragmentation area along the track length. The (Zr, Nb)N coating demonstrated relatively low critical load, which was probably associated with the formation of tensile stresses in the ZrN-based solid solution. A comparison with the data obtained earlier, showed that a decrease in the niobium concentration in the (Zr, Nb)N coating and increase in the hafnium concentration in the (Zr, Hf)N coating led to the higher critical load Lc3.

Funding This work was financially supported by the Belarusian Republican Foundation for Fundamental Research (Project No. T23RNF-228) and the Russian Science Foundation (Project No. 23-49-10038).

Author Contribution Conceptualization N.N.Ch., S.N.G. and A.A.V.; methodology N.N.Ch., A.V.B., N.V.B. and D.P.R.; formal analysis and investigation N.N.Ch., A.V.B., N.V.B., O.V.R., A.Yu.I., D.P.R, A.K.K., V.V.U., V.V.Ch. and I.A.S.; writing N.N.Ch. and A.A.V.; funding acquisition N.N.Ch., S.N.G., A.A.V.; supervision N.N.Ch., S.N.G. and A.A.V. All authors have read and agreed to the published this version of the manuscript.

Data availability Data will be made available on request.

Conflicts of interest The authors declare that they have no known competing financial interests or personal relationships that could have appeared to influence the work reported in this paper.

References

1. Chen, Q., Thouas, G.A.: Metallic implant biomaterials. Mater. Sci. Eng. R **87**, 1–57 (2015). https://doi.org/10.1016/j.mser.2014.10.001
2. Kaur, M., Singh, K.: Review on titanium and titanium based alloys as biomaterials for orthopaedic applications. Mater. Sci. Eng. C **102**, 844–862 (2019). https://doi.org/10.1016/j.msec.2019.04.064
3. Chen, H., Feng, R., Xia, T., Wen, Z., Li, Q., Qiu, X., Huang, B., Li, Y.: Progress in surface modification of titanium implants by hydrogel coatings. Gels **9**, 423 (2023). https://doi.org/10.3390/gels9050423

4. Grabovetskaya, G.P., Stepanova, E.N., Zabudchenko, O.V., Mishin, I.P.: Formation of the structure and properties of the near-surface layer in alloys of the Ti–6Al–4V–H system under irradiation with a pulsed electron beam. Russ. Phys. J. **66**, 172–179 (2023). https://doi.org/10.1007/s11182-023-02922-3
5. Gabor, R., Cvrček, L., Kudrnová, M., Hlinka, J., Večeř, M., Buřil, M., Walter, J., Čekada, M., Drnovšek, A., Unucka, P., Mamulová Kutláková, K., Motyka, O., Seidlerová, J.: ZrN coating as a source for the synthesis of a new hybrid ceramic layer. Appl. Surf. Sci. Adv. **22**, 100615 (2024). https://doi.org/10.1016/j.apsadv.2024.100615
6. Rabadzhiyska, S., Dechev, D., Ivanov, N., Ivanova, T., Strijkova, V., Katrova, V., Rupetsov, V., Dimcheva, N., Valkov, S.: Wear and corrosion resistance of ZrN coatings deposited on Ti6Al4V alloy for biomedical applications. Coatings **14**, 1434 (2024). https://doi.org/10.3390/coatings14111434
7. Wu, X., Han, H., Jiang, Y., Zhu, D., Zuo, B., Bian, S., Chen, C., Zhao, L., Xu, J., Yu, L.: Opportunities and challenges of the nitride coatings for artificial implants: A review. Surf. Coat. Technol. **480**, 130587 (2024). https://doi.org/10.1016/j.surfcoat.2024.130587
8. Savostikov, V.M., Leonov, A.A., Denisov, V.V.: Formation of a Zr+ZrxNy+(Zr+TiBSiNi)N+(TiBSiNi)N gradient-layered coating based on physical and tribotechnical characteristics of constituent layers. Russ. Phys. J. **67**, 1090–1099 (2024). https://doi.org/10.1007/s11182-024-03220-2
9. Kanoun, M., Goumri-Said, S.: Effect of alloying on elastic properties of ZrN based transition metal nitride alloys. Surf. Coat. Technol. **255**, 140–145 (2014). https://doi.org/10.1016/j.surfcoat.2014.03.048
10. Zhang, S., Wang, N., Li, D.J., Dong, L., Gu, H.Q., Wan, R.X., Sun, X.: The synthesis of Zr–Nb–N nanocomposite coating prepared by multi-target magnetron co-sputtering. Nucl. Instrum. Methods Phys. Res. Sect. B **307**, 119–122 (2013). https://doi.org/10.1016/j.nimb.2012.12.067
11. Wu, Z.T., Qi, Z.B., Jiang, W.F., Wang, Z.C., Liu, B.: Influence of niobium addition on microstructure, mechanical properties and oxidation resistance of ZrN coatings. Thin Solid Films **570**, 256–261 (2014). https://doi.org/10.1016/j.tsf.2014.05.019
12. Krysina, O.V., Ivanov, Yu, F., Prokopenko, N.A., Shugurov, V.V., Petrikova, E.A., Denisova Yu, A., Tolkachev, O.S.: Influence of Nb addition on the structure, composition and properties of single-layered ZrN-based coatings obtained by vacuum-arc deposition method. Surf. Coat. Technol. **387**, 125555 (2020). https://doi.org/10.1016/j.surfcoat.2020.125555
13. Qian, J., Zhou, F., Li, K., Wang, Q., Kong, J., Zhou, Z.: Optimization of deposition parameters and performance analysis of Nb-Zr-N composite films. Surf. Coat. Technol. **466**, 129641 (2023). https://doi.org/10.1016/j.surfcoat.2023.129641
14. Atar, E., Kayali, E.S., Cimenoglu, H.: Sliding wear behaviour of ZrN and (Zr, 12 wt.% Hf)N coatings. Trends Plant Sci. **39**, 297–302 (2006). https://doi.org/10.1016/j.triboint.2005.01.038
15. Atar, E., Kayali, E.S., Cimenoglu, H.: Reciprocating wear behaviour of (Zr, Hf)N coatings. Wear **257**, 633–639 (2004). https://doi.org/10.1016/j.wear.2004.03.005
16. Atar, E., Cimenoglu, H.C., Kayali, E.S.: Hardness characterisation of thin Zr(Hf, N) coatings. Surf. Coat. Technol. **162**, 167–173 (2003). https://doi.org/10.1016/S0257-8972(02)00558-3
17. Atar, E., Sarioglu, C., Cimenoglu, H., Kayali, E.S.: Residual stresses in (Zr, Hf)N films (up to 11.9 at.% Hf) measured by X-ray diffraction using experimentally calculated XECs. Surf. Coat. Technol. **191**, 188–194 (2005). https://doi.org/10.1016/j.surfcoat.2004.02.024
18. Cherenda, N.N., Grigoriev, S.N., Basalai, A.V., Petukh, A.B., Vereschaka, A.A., Reva, O.V., Isobello, Yu, A., Rusalsky, D.P., Kuleshov, A.K., Uglov, V.V.: Comparative study of mechanical and corrosion properties of coating on the basis of ZrN and TiN solid solutions. High Temp. Mater. Process. (new york) **29**(3), 35-55 (2025). https://doi.org/10.1615/HighTempMatProc.2024057613
19. Vereschaka, A., Cherenda, N., Sotova, C., Uglov, V., Reva, O., Basalai, A., Isobello, A., Baranova, N.: Development of multicomponent nanostructured nitride coatings to protect against corrosion products from titanium alloy. Coatings **13**, 2028 (2023). https://doi.org/10.3390/coatings13122028
20. Cherenda, N.N., Petukh, A.B., Kuleshov, A.K., Rusalsky, D.P., Bibik, N.V., Uglov, V.V., Grigoriev, S.N., Vereschaka, A.A., Astashynski, V.M., Kuzmitski, A.M.: Scratch testing of ZrN coating on Ti-6Al-4V titanium alloy surface preliminary treated by compression plasma flows impact. High Temp. Mater. Process. (new york) **28**(3), 25–36 (2024). https://doi.org/10.1615/HighTempMatProc.2023051420

Authors and Affiliations

N. N. Cherenda[1] · S. N. Grigoriev[2] · A. V. Basalai[3] · N. V. Bibik[1] · A. A. Vereschaka[4] · A. Yu. Isobello[3] · D. P. Rusalsky[1] · A. K. Kuleshov[1] · V. V. Uglov[1] · V. V. Chayeuski[5] · I. A. Saladukhin[5]

✉ N. N. Cherenda
cherenda@bsu.by

S. N. Grigoriev
s.grigoriev@stankin.ru

A. V. Basalai
anna.basalay@mail.ru

N. V. Bibik
nvbibik@bsu.by

A. A. Vereschaka
dr.a.veres@yandex.ru

A. Yu. Isobello
AIzobello@phti.by

D. P. Rusalsky
rusalsky@bsu.by

A. K. Kuleshov
kuleshak@bsu.by

V. V. Uglov
uglov@bsu.by

V. V. Chayeuski
v.chaevskij@bsuir.by

I. A. Saladukhin
i.solodukhin@bsuir.by

[1] Belarusian State University, Minsk, Belarus

[2] The Moscow State University of Technology “STANKIN”, Moscow, Russian Federation

[3] Physico-Technical Institute of the National Academy of Sciences of Belarus, Minsk, Belarus

[4] Institute for Design-Technological Informatics of the Russian Academy of Sciences, Moscow, Russian Federation

[5] Belarusian State University of Informatics and Radioelectronics, Minsk, Belarus